

# APPLYING THE STRENGTH REDUCTION METHOD TO STUDY OF STABILITY OF RESIDUAL MOUNTAINS: A PARTICULAR APPLICATION

---

**Xin Jin\***

College of Art and Design, Shaanxi University of Science and Technology, Xi'an, Shaanxi, 710021, China

[wjxin@sust.edu.cn](mailto:wjxin@sust.edu.cn)

**Yucheng Hua**

College of Art and Design, Shaanxi University of Science and Technology, Xi'an, Shaanxi, 710021, China

**Qiao Tang**

College of Art and Design, Shaanxi University of Science and Technology, Xi'an, Shaanxi, 710021, China



**Reception:** 31/11/2022 **Acceptance:** 26/11/2022 **Publication:** 21/01/2023

## Suggested citation:

J., Xin, H., Yucheng and T., Qiao. (2023). **Applying the strength reduction method to study of stability of residual mountains: A particular application.** *3C Tecnología. Glosas de innovación aplicada a la pyme*, 12(1), 33-52. <https://doi.org/10.17993/3ctecno.2023.v12n1e43.33-52>

## ABSTRACT

*Due to huge disaster-caused force, seismic geological disasters primarily induce residual landslide, collapse and debris flow disasters with far higher hazard extent than that of earthquake disasters. Wherefore, this paper, with various vibration slopes caused by the most representative Wenchuan earthquake as research objects, introduces the strength reduction method to the stability study of residual mountains in a certain area, puts forward dynamic stability slope evaluation method based on dynamic and overall strength reduction method to obtain the mountain slope stability situation in the process of gradual instability, searches out the sliding surface of progressive expansion making use of dynamic strength reduction method and calculates dynamic safety index in the process of gradual slope instability pursuant to the calculation advantages of dynamic strength reduction method, so as to realize the analysis and regulation of the whole process of slope instability. The results show that in the stability analysis of a homogeneous slope, the safety index of slope stability calculated by strength reduction method is 6.7%, 8.8% and 10.5% higher than that calculated by finite element limit equilibrium method, Bishop method and Janbu method respectively. In the stability analysis of a multi-layer soil slope, the safety index of slope stability calculated by strength reduction method is 4.8%, 4.3% and 9.4% higher than that calculated by other three algorithms. While in the stability analysis of soft interlining slope, the safety indexes of slope stability calculated by the method proposed in this paper are increased by 26.10%, 29.11% and 26.46% respectively compared with other three algorithms, indicating that the stability of landslide residual mountains calculated by strength reduction method proposed in this paper is the highest.*

## KEYWORDS

*Strength reduction method; Landslide residual mountain; Stability study; Safety index; Sliding surface*

## PAPER INDEX

ABSTRACT

KEYWORDS

1. INTRODUCTION

2. FAILURE CHARACTERISTICS OF MOUNTAIN SLOPES AND IMPROVEMENT OF STRENGTH REDUCTION METHOD

2.1. Deformation and failure characteristics of residual slope after landslide

2.2. Actual failure process of mountain slope

2.3. Sliding surface search based on dynamic strength reduction

3. DYNAMIC STABILITY ANALYSIS OF MOUNTAIN SLOPE BASED ON STRENGTH REDUCTION METHOD

4. RESULTS AND ANALYSIS

4.1. Landslide residual mountain conditions in a certain area

4.2. Experiment parameters of mountain slope in a certain area

4.3. Compare with the results of different algorithms

5. DISCUSSION

6. CONCLUSION

7. DATA AVAILABILITY STATEMENT

REFERENCES

CONFLICT OF INTEREST

# 1. INTRODUCTION

In mountainous and hilly areas, landslides are more common, and similar to earthquakes, mudslides and other disasters, generally have relatively large hazard extent. In the vast land area of China, the geographical conditions are relatively complex, and the landslide areas are widely distributed, especially in the mountainous areas of southwest, northwest, and east China [1-2]. When a landslide occurs, partial or whole pieces of land will appear one after another in a relatively slow speed and a relatively long cycle, and will intermittently slide. [3-4].

Landslides are extremely harmful, especially that large-scale landslides can destroy entire villages, cut off rivers, destroy farmland and forests, and even damage the safety of life and property of people and countries to a large extent, seriously hindering and destroying the construction process of countries [5]. Landslides in China have the characteristics of various types, large scale, wide distribution, strong concealment and strong destructiveness, and most landslides are sudden and unpredictable, which brings serious harms to the society [6].

In this regard, it is of great significance to implement monitoring and early warning of landslides. Landslide movement is highly complex and is affected by many factors. At present, it is difficult to thoroughly understand the internal characteristics of each landslide, and to accurately predict each landslide [7-9]. However, landslide monitoring helps to master and analyze the evolution and characteristics of landslide mass. With the continuous progress of landslide monitoring technology, in order to obtain more detailed landslide data, a more in-depth understanding of landslides can be obtained [10-12].

In recent years, many foreign researchers have carried out research on rock mechanics algorithms. For example, the literature [13] introduced the concept of damage mechanics in the metal creep fracture research and rock mechanics research for the first time. The literature [14] used the concept of fracture surface to theoretically discuss the continuous damage behavior of rock and concrete. Since then, people have established various damage theories based on different damage mechanisms and basic theories, and applied them to the study of nonlinear, plastic, and viscoplastic damage of rock materials. The literature [15] first applied the damage theory to establish damage mechanics model of rock-concrete continuum. The literature [16] established corresponding models and theories based on the structural characteristics of the rock itself. The literature [17] proposed the famous "strain equivalence hypothesis", which laid the foundation for the study of damage theory. The literature [18] proposed a new elastic-plastic damage model based on irreversible thermodynamics and damage mechanics, which comprehensively considered plastic friction deformation and plastic pore deformation, and adopted damage variables to describe the development of microscopic defects. The literature [19] defined a damage variable as the second-order tensor of fracture density, took into account the damage evolution of this damage variable pursuant to fracture propagation, and thereby established a corresponding damage model. Based on the homogenization theory, whereafter, a thermodynamic framework for the meso-mechanical damage model was built. Zhu Qizhi et al. reckoned that the rock was a heterogeneous material composed

of an elastic solid matrix and fractures, and proposed a corresponding meso-mechanical damage model. The literature [20], on the basis of considering the dynamic propagation of micro-fractures, proposed a corresponding meso-mechanical model of rock damages, believing that the stress-strain curve, failure strength and damage development rate of rocks were closely related to the friction index, initial fracture length and loading rate. The literature [21] came up with a micro-fracture damage model of brittle rock under uniaxial compression load as well as theories of micro-fracture fracture mechanics and rock damage mechanics based on the assumption of random distribution of micro-fractures. To be concrete, the mechanical properties under the load were analyzed, that is, when the external load reached a certain level, the micro-fractures began to expand, the mechanical properties of the rock changed, and until the macro-fracture of the rock occurred, the fracture growth rate increased with the external load.

With the in-depth research aiming at foreign researchers, domestic scholars have also carried out research on the stability of rock and soil slopes. For instance, based on the principle of object balance, the literature [22] proposed a finite sliding displacement evaluation method of slope stability according to slope potential deformation, in which the force exceeding the yield resistance of the sliding body is used as the calculation standard for the occurrence of the slope and landslide. The literature [23] used the FLAC valuation method of slope stability according to slope potential deformation, and carried out the research of seismic slope failure mechanism combined with the seismic slope numerical simulation software with both tensile and shear failure functions. Through analysis, it was concluded that the failure of the seismic slope was composed of the upper tensile failure and the lower shear failure of the potential rupture zone, and the method for determining the location of the rupture surface of the earthquake slope was given through various means. The literature [24] performed a large number of on-site investigations. Precisely, on the basis of aforementioned above, the special instability phenomena such as vibration collapse and high-speed ejection of the slope under the strong earthquake load were studied, and the genesis mechanism of earthquake-triggered collapse and landslide was classified according to the specific slope structure. Moreover, a calculation program for the safety index of a landslide numerical simulation software with both tensile was proposed to study the stability of slopes under the condition of known sliding surfaces, and a comparative discussion between the traditional seismic slopes was carried out via FLAC 3D displacement evaluation method. From a mesoscopic approach, the literature [26] studied the instability mode of slopes via a strength reduction calculation module in the RFPA software. The literature [27] discussed the strength reduction method and proposed a more reasonable reduction calculation method, which promoted actual use numerical simulation software with both tensile. With the deepening of research, there are more and more improved algorithms for strength reduction. However, numerous studies have found that in order to study the stability of residual mountains, it urgently requires to take into account the shear-tensile composite yield criterion of mountains, as well as single static safety index, principal stress and cohesion of mountain slopes. For this, numerical simulation software with both tensile did calculate damaged area of the mountain slope [28-30],

but did not consider the soil layer of the mountain slope. Not all the soil layers of the mountains are homogeneous, and some soil layers are multi-layer soil or contain weak inter-layers, so it is very necessary to study the stability of the residual mountain according to the conditions of different soil layers.

Pursuant to the fact that the general algorithm does not take into account the pull fracture and further study landslide residual mountains, in this paper, the shape change and structural damage characteristics of the residual slopes on the rear wall of the landslide is analyzed, and the sliding surface searching of progressive expansion is implemented making use of dynamic strength reduction method. At the same time, the residual slope of the rear wall of a landslide in a certain area is also a typical representative and epitome of the many shaking slopes of the "5.12" Wenchuan earthquake. It can be predicted that in the next 3 to 5 years, it will be a period of high incidence of collapse, landslides and debris flows in earthquake-stricken areas. The research ideas, methods and understanding of its post-earthquake stability will also provide guidance and reference for the evaluation of similar slopes in earthquake-stricken areas.

## **2. FAILURE CHARACTERISTICS OF MOUNTAIN SLOPES AND IMPROVEMENT OF STRENGTH REDUCTION METHOD**

### **2.1. DEFORMATION AND FAILURE CHARACTERISTICS OF RESIDUAL SLOPE AFTER LANDSLIDE**

According to the interpretation of low-altitude aerial photography near the residual mountain on the rear wall of a landslide in a certain area by helicopter, and combined with on-site geological mapping, it shows that after the "5.12" earthquake, there are mainly three groups of fractures on the surface of the entire back-edge mountains[31]. And the distribution of residual mountains and fractures on the rear wall of the landslide is primarily: (1)  $N40^{\circ}\sim 50^{\circ}E$  and  $N70^{\circ}E\sim EW$  direction, this group of fractures is mainly consistent with the boundary of the rear wall of a landslide in a certain area, with an extension length of about  $20\sim 200m$  and; (2)  $N10^{\circ}W\sim$  near SN direction  $\sim N10^{\circ}E$ , this group of fractures is the same as the main direction of the Dashuigou and Xiaoshuigou valleys, with an extension length of about  $50\sim 400m$ , and showing that unloading and tension are towards the free surface of the big and small ditches, but the scale of the side of the small ditch is obviously small; (3)  $N70^{\circ}W$  direction, this group of fractures are distributed on the ridge line of the highest watershed and are consistent with the trend of the ridge line, with an extension length of about about  $1000m$  and belonging to the earthquake-vibration fractures on the steep slope of the ridge [32].

The above-mentioned fractures are all extensional, with an opening width of 10-50 cm. Since the penetration depth of each fracture cannot be measured, according to the earthquake in the core area (such as Dujiangyan, Yingxiu, Wolong, Beichuan,

Qingchuan, etc.), the characteristics of the slope seismic effect (that is, the slope slump effect caused by the earthquake on the thin ridge with a slope gradient of obviously more than  $50^\circ$  and without deep tensile fracture) are adopted to predict the distribution of the residual mountain mass on the rear wall of the landslide in a certain area. The depth of the pull fracture is generally between 10 and 50m. Except for the  $N40^\circ-50^\circ$  E group fractures near the front edge of the mountain, which has penetrated into the weakly weathered rock body, the rest of the fractures near the ridge line are expected to be a deep location within the strongly weathered rock body. [33].

Judging from the distribution of the above-mentioned three groups of fractures with different extension directions and scales, the shallow surface layer of the entire residual mountain has basically been disturbed as a whole. Instead, collapse, slide and pull fractures also occur in the direction of large and small ditches, but the former has more advantages. Although the superficial integrity of the residual mountain has been basically completely destroyed, the integrity of the underlying weakly weathered rock mass has remained basically intact.

## 2.2. ACTUAL FAILURE PROCESS OF MOUNTAIN SLOPE

The slope instability is a gradual process that evolves from part to the whole, rather than an instant process. Because of existence of weak surface, the mechanical index of mountain slope decreases due to rainfall, the load distribution is unbalanced and local stress concentration occurs, thereby resulting in some elements are damaged first [34]. Slowly, the principal stress will continue to extend and adjust its own concentration after the internal components is damaged, regrouping into a stress region. At this time, the damage area of the mountain structure increases and converges, and finally becomes a complete mass through sliding surface. Figure 1 shows the whole process of slope damage.

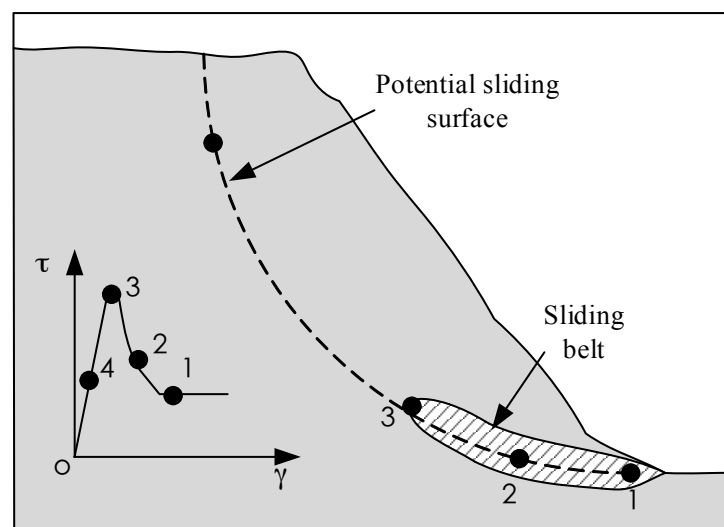


**Figure 1.** Schematic diagram of progressive failure of mountain slope

In Figure 1, at points 1 and 2, if the shear force is greater than that of the peak point, the mechanical index will decrease due to rainfall,. At this time, it can be



regarded as that the shear stress at point 3 has just peaked, and the shear stress at point 4 is well below the peak value. Moreover, since the sliding belt will continue to expand, the stress will be completed at point 4, the highest point will be completed at point 4, and at the same time, a complete sliding surface will be formed. Obviously, when the sliding zone is produced, its strength value will change from the highest point to the lowest point. In this way, the whole process can improve the characteristics of the formation of the Osian sliding zone.

The damage of slope structure and the process of landslide are not sudden, but gradual. Also, the slope instability is a gradual unsuccessful process, so it is necessary to reflect the whole gradual process of slope stability for evaluation [35]. If the strength value of the slope instability is wanted to decrease, strength reduction calculation will cause the final plastic zone to be too large.

### 2.3. SLIDING SURFACE SEARCH BASED ON DYNAMIC STRENGTH REDUCTION

The whole process deformation characteristics of geotechnical materials are mainly classified into two types, namely "hardening" and "softening". Regarding the shape change and mechanism damage characteristics of the sliding belt in the unsafe process of mountain slope, relevant researchers have verified via theory and experiments that the sliding belt of the slope has softening characteristics. Thus, the slope stability analysis must take into account the strain softening characteristics of geotechnical materials [36].

Based on referred strength reduction criteria and softening characteristics of the sliding belt, some scholars first proposed a calculation method and then obtained the parameters for reducing the local slope strength cohesion and internal friction angle, as shown in Figure 2

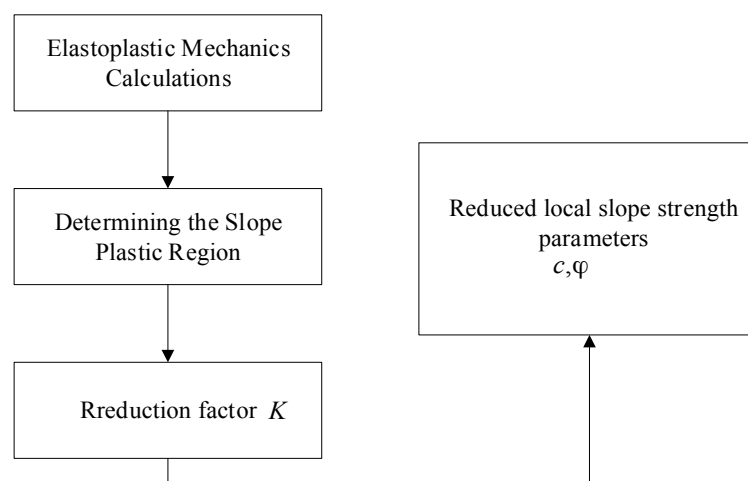


**Figure 2.** Strength reduction calculation process

Figure 2 shows the strength reduction process in detail, in which the minimum value of principal stress calculated is the same as the value of tensile failure strength. Concretely, it is first to destroy the reduction element index, and then obtain the



parameters for reducing the local slope strength cohesion and internal friction angle, so as to perform mechanical calculation aiming at the slope plastic region. Assuming that the deformation strength characteristics of the sliding zone geotechnical materials conform to the ideal elastic-plastic softening model, by calculating the damaged area of the mountain slope according to the elastic-plastic criterion, it is found that the area of slope increases slowly, which stops when the slope state reaches the limit equilibrium [37].

Tensile failure often occurs in a certain range of landslide crest, so after determining mechanical strength parameters of the sliding belt shear yielding, it is very necessary to integrate the Mohr Coulomb tensile failure model into the numerical study, that is, if the minimum value of principal stress is the same as the value of tensile failure strength, the rock and soil mass will suffer unsafe state process. Tensile composite yield criterion can be expressed as:

$$F^t = \sigma_3 - \sigma_t = 0 \quad (1)$$

A single static safety index can be expressed as:

$$F^s = \sigma_1 - \frac{1 + \sin \varphi}{1 - \sin \varphi} \sigma_3 + \frac{2c \cos \varphi}{1 - \sin \varphi} = 0 \quad (2)$$

In the above formulas,  $\sigma_1$  and  $\sigma_3$  are the maximum and minimum principal stresses, respectively;  $c$  is the cohesion force;  $\varphi$  is the internal friction angle; and  $\sigma_t$  is the tensile strength.

The tensile strength of the slope is basically unchanged, so the tensile strength is not reduced in the strength reduction method [38-39]. Only under the conditions that earthquake and other basic factors work, the tensile strength of the slope will be and needs to be reduced. When calculating the damaged area of the slope according to the elastic-plastic criterion, the mechanical strength parameter of the sliding belt is narrowed by the reduction factor  $K$ , that is:

$$\left\{ \begin{array}{l} c_{loc} = \frac{c}{K} \\ \varphi_{loc} = \arctan \frac{\tan \varphi}{K} \end{array} \right\} \quad (3)$$

In the above formula,  $c_{loc}$  and  $\varphi_{loc}$  are the cohesion force and the internal friction angle of the local damaged area, respectively

### 3. DYNAMIC STABILITY ANALYSIS OF MOUNTAIN SLOPE BASED ON STRENGTH REDUCTION METHOD

From the above data research and actual operation, it is obvious that whether the slope is safe and stable as time goes by, the whole process of the slope from local

failure and gradual development to overall instability will change dynamically, experiencing stable, less stable and unstable evolutionary processes.

The steps for evaluating the dynamic stability of mountain slopes are shown in Figure 3.

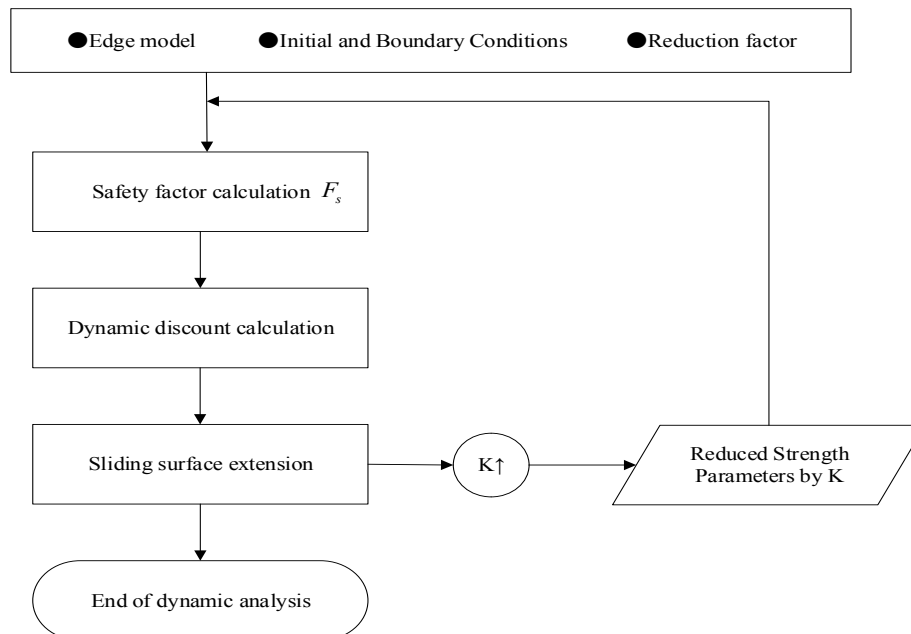


**Figure 3.** Dynamic evaluation process of mountain slope stability

In the traditional slope stability evaluation method, a single static safety index  $F_s$  is used to evaluate the slope stability, but the static safety index  $F_s$  is not conducive to the stability analysis and regulation of landslide disasters. Therefore, this paper proposes that the safety index  $F_s$  is a dynamic stability evaluation index.

(1) When the plastic zone appears in the local element of the mountain slope, the mechanical parameters of the element in the plastic zone are reduced to indicate that the strength of the local element softens and decreases.

(2) The overall strength reduction method and formula (4) are adopted to reduce the strength parameters  $c$  and  $\varphi$ , of the entire slope. The reduction range includes not only the softened plastic zone, but also the unyielding slope. For the plastic zone in step (1), the softened parameter value is reduced. When the reduction reaches a sudden change in the slope displacement, the safety index  $F_s$  in the current state is obtained.

(3) According to Figure 3, after the strength parameters  $c$  and  $\varphi$  are reduced, the elastoplastic mechanical balance calculation is carried out. Since the elements around the plastic zone of stress concentration will generate a new plastic zone, the plastic zone elements will increase.

(4) The increase of plastic zone elements indicates the expansion of the slope sliding surface. At this time, the mechanical parameters of the newly formed sliding surface are reduced according to steps (1) and (3).

(5) According to step (2), the slope safety index  $F_s$  is obtained after sliding surface expansion.

(6) The dynamic and overall strength reduction method is used to repeat the above steps to obtain a series of dynamic safety indexes, stop the reduction after the sliding surface is penetrated, and finish dynamic security and stability evaluation of the slope.

In order to track the evolution law of the slope safety index  $F_s$  in the whole process, this paper, combined with the advantages of dynamic strength reduction method, selects a representative section to study how to bring the strength reduction calculation method into the analysis of slope dynamic safety and stability state, in which the possibility of overall landslide occurrence is small in the gradual failure process of the slope, but the reduction index  $K$  obtained by the dynamic strength reduction method does not represent the safety index of the slope (as  $K$  in equation (3)), only representing the degree of reduction. Therefore, the dynamic and overall strength reduction calculation methods are combined to analyze the slope stability, and slowly enter the unsafe state process, thereby obtaining the safety index via calculation, and obtaining the stability state of the slope on the basis of the safety index.

Concretely, the fractures at an overall back-edge mountain are dislocated to reduce and a representative section is selected as the entire slope, so as to obtain the safety index  $F$  under the limit state, that is:

$$\left\{ \begin{array}{l} c' = \frac{c}{F} \\ \varphi' = \arctan \frac{\tan \varphi}{F} \end{array} \right\} \quad (4)$$

In the formula,  $c'$  and  $\varphi'$  are the reduced cohesion force and the internal friction angle, respectively.

## 4. RESULTS AND ANALYSIS

### 4.1. LANDSLIDE RESIDUAL MOUNTAIN CONDITIONS IN A CERTAIN AREA

In a certain area, there is still a mountain with a vertical length of 460-500m and a horizontal width (between the big water ditch and the small water ditch) of 460-640 m at the rear wall of the landslide, which is characterized by a steep front edge and a gentle back edge. The slope of the front edge (that is, the rear wall of the landslide in a certain area) is about 45°, and the back edge is the original slope with a gentle slope of 10° to 15°. It can be seen via qualitative analysis that the residual mountain mass on the rear wall of a landslide in a certain area will be dominated by local sporadic collapse and slump in the superficial part, and the possibility of overall landslide occurrence is small. Therefore, in the quantitative calculation of stability, the

possible sliding surface is formed based on the most unfavorable residual mountain slope structure and its various structural surfaces, which is regarded as the controlling boundaries for quantitative calculations of stability. At the same time, the various residual mountain slopes and superficial residual mountain slopes formed due to the earthquake will obviously serve as the boundary of the back edge tensile fracture.

Based on comprehensive analysis, it can be inferred that the residual mountain may have a large-scale failure mode: the back edge through fractures are dislocated → the middle layer slides → the front edge shear failure occurs, so it can also be attributed to a three-stage mechanism of tension cracking-sliding-shearing. Among them, the front edge of the slope crest is most likely to collapse.

## 4.2. EXPERIMENT PARAMETERS OF MOUNTAIN SLOPE IN A CERTAIN AREA

According to the geological prototype, geometric mode of right bank is built, and to perform stability calculation, a representative section is selected. Specifically, the section model of the computational mesh model is set to be 478m long and 470m high, and the total number of elements and nodes is 44695 and 71396 respectively. The rock-material constitutive model adopts the Mohr Coulomb rule for the most suitable elastic-plastic model criterion. The mechanical parameters of the three kinds of rock dikes in the corresponding stratum distribution on the vertical surfaces on the left and right sides, and fixed constraints on the bottom boundary are determined respectively.

Combined with the exposed shape of the section, the slope mass is generalized as *V2*, *V1*, *IV*, *III2*, *III1* and *II* rock-soil mass and concrete after support (C25 strength grade), and the mechanical parameters of the three kinds of rock dikes in the corresponding stratum distribution are the same as IV-type rock mass. The natural bulk density, elastic model and Poisson's ratio appearing in this experiment are all measured by measuring instruments before the experiment. The layer parameter values are shown in Table 1.

**Table 1.** Parameters of the calculation model for the slope on the right side of the residual mountain.

| Medium                  | Natural test weight / (kN•m <sup>-3</sup> ) | Elastic Modulus /Gpa | Poisson's ratio | Cohesion /Mpa | Internal friction angle / (°) |
|-------------------------|---|----------------------|-----------------|---------------|-------------------------------|
| f231                    | 25.8  | 2.0                  | 0.28            | 0.9           | 22.8                          |
| Deep unloading fracture | 26.2  | 2.0                  | 0.28            | 2.0           | 36.0                          |
| V2 class                | 22.1  | 2.0                  | 0.27            | 1.8           | 21.8                          |
| V1 class                | 24.5  | 4.0                  | 0.27            | 2.0           | 26.5                          |
| IV class                | 25.8  | 6.0                  | 0.26            | 7.0           | 38.6                          |

|            |      |     |      |      |      |
|------------|------|-----|------|------|------|
| III1 class | 26.2 | 8.0 | 0.24 | 15.0 | 50.2 |
| III2 class | 26.2 | 7.5 | 0.23 | 17.5 | 51.3 |
| III class  | 26.5 | 9.0 | 0.22 | 20.0 | 52.5 |

In Table 1, a total of 87 groups of physical and mechanical tests of rock blocks have been completed on the residual mountain. The values of mechanical parameters are comprehensively determined on the basis of indoor and outdoor tests, combined with engineering analogy and parameter inversion.

For a homogeneous slope in mountains at a certain area, its geometric model is shown in Figure 4, and its material property parameters are shown in Table 2.

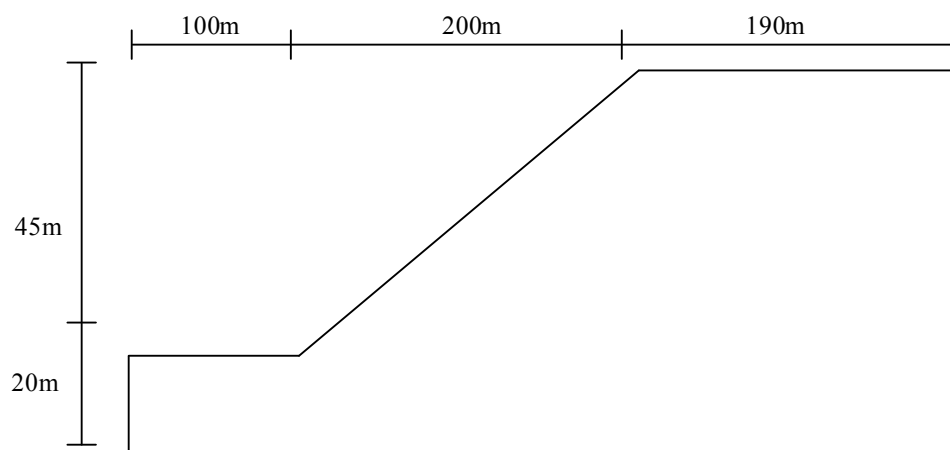


**Figure 4.** Geometric model of the homogeneous slope of the mountain

**Table 2.** Soil parameters of mountain homogeneous slope

| c/kPa | $\phi/(^{\circ})$ | $\gamma/(\text{kN}/\text{m}^3)$ | E/Mpa | $\nu$ |
|-------|-------------------|---------------------------------|-------|-------|
| 3     | 19.6              | 20                              | 10    | 0.25  |

Midas GTS NX is a kind of software that can analyze soil layers and tunnel structures, which can carry out various analysis of related mountains, strata, soil layers and tunnels, such as the mechanical parameter analysis of the three kinds of rock dikes in the corresponding stratum distribution, as well as solid structure and type analysis, with fast analysis speed, excellent graphics and output capabilities. Therefore, in this study, Midas GTS NX software is adopted to analyze the stability of three kinds of residual mountain slopes using the finite element limit equilibrium method, Bishop method, Janbu method and the mountain slope calculation model designed herein based on the strength reduction method in order.

The geometric model and material property parameters of a multi-layer soil slope on a mountain in a certain area are shown in Figure 5, and Table 3 respectively.

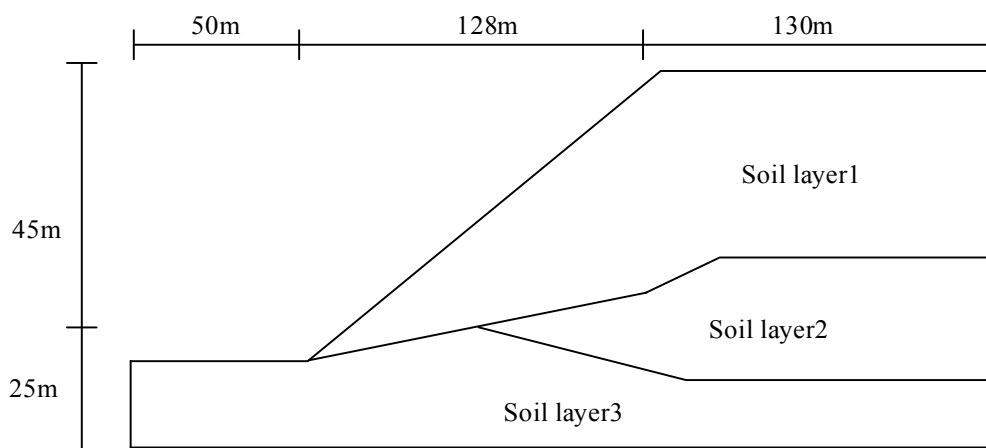


**Figure 5.** Geometric model of a multi-layer soil slope in mountain

**Table 3.** Soil parameters of a multi-layer soil slope in mountain

| Soil layer | c/kPa | $\phi/(\text{°})$ | $\gamma/ (\text{kN/m}^3)$ | E/Mpa | $\nu$ |
|------------|-------|-------------------|---------------------------|-------|-------|
| 1          | 0     | 38.0              | 19.5                      | 10    | 0.25  |
| 2          | 5.3   | 23.0              | 19.5                      | 10    | 0.25  |
| 3          | 7.2   | 20.0              | 19.5                      | 10    | 0.25  |

The geometric model and material property parameters of a soft interlining slope in a certain area are shown in Figure 6, and Table 4 respectively.

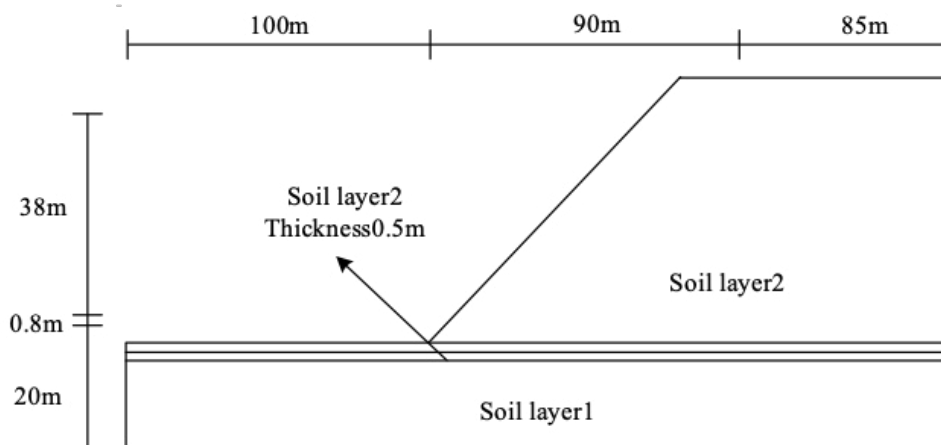


**Figure 6.** Geometric model of a weak interlining slope in mountain

**Table 4.** Soil parameters of a weak interlining slope in mountain

| Soil layer | c/kPa | $\phi/(\text{°})$ | $\gamma/ (\text{kN/m}^3)$ | E/Mpa | $\nu$ |
|------------|-------|-------------------|---------------------------|-------|-------|
| 1          | 28.5  | 20.0              | 18.84                     | 60    | 0.25  |
| 2          | 0     | 10.0              | 18.84                     | 20    | 0.25  |

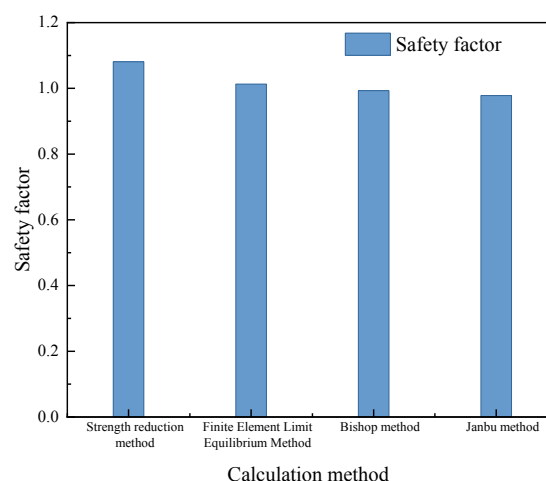
### 4.3. COMPARE WITH THE RESULTS OF DIFFERENT ALGORITHMS

The calculation results of slope stability are shown in Figure 7 in detail.

After the stability of a homogeneous slope in a certain area is calculated by the finite element limit equilibrium method, the Bishop method, the Janbu method and the mountain slope calculation model designed in this paper according to the mechanical parameters of the three kinds of rock dikes in the corresponding stratum distribution, it is obvious from Figure 7 (a) that, in a certain area, the maximum safety index calculated via mountain slope calculation model designed in this paper is 1.081, while the maximum safety index calculated by the finite element limit equilibrium method is 1.013, the maximum safety index calculated by the Bishop method is 0.993, and the maximum safety index calculated by the Janbu method is 0.978, indicating that the slope stability safety index of a homogeneous slope in a certain area calculated by mountain slope calculation model is increased by 6.7%, 8.8% and 10.5% compared with that calculated by finite element limit equilibrium method, Bishop method and Janbu method respectively.

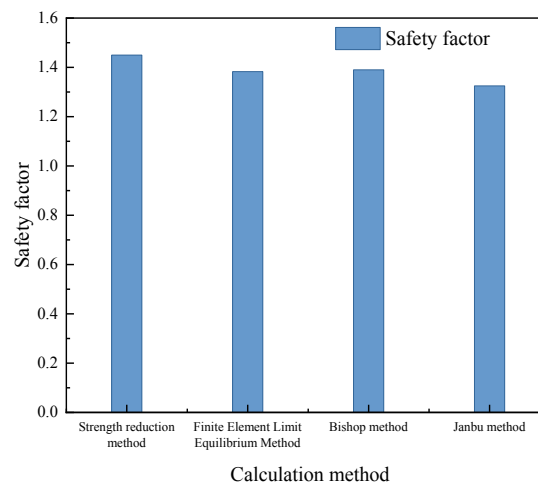
Similarly, in the stability analysis of a multi-layer soil slope, the maximum safety index calculated by mountain slope calculation model designed in this paper is 1.450, while the maximum safety index calculated by the finite element limit equilibrium method, Bishop method and Janbu method is 1.390, 1.383, and 1.325 successively, indicating that the slope stability safety index of a multi-layer soil slope calculated by strength reduction method is 6.7%, 8.8% and 10.5%. higher than that calculated by finite element limit equilibrium method, Bishop method and Janbu method. The concrete results is as shown in Figure 7(b)

Again, as can be seen from Figure 7(c), in the stability analysis of a weak interlining slope, the safety index calculated by the finite element limit equilibrium method is 1.027, the safety index calculated by the the Bishop method is 1.003., and the safety index calculated by the Janbu method is 1.024. Compared with other three algorithms, the safety index of slope stability calculated by strength reduction method is increased by 26.46%, 29.11% and 26.10% respectively.

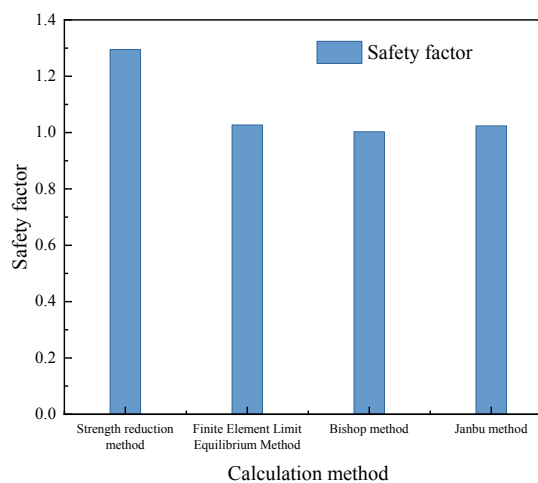




## (a) Calculation results of the stability of the homogeneous slope of the mountain



## (b) Calculation results of the stability of the multi-layer soil slope in the mountain



## (c) Calculation results of stability of mountain slope with weak interlayer

**Figure 7.** The results of the mountain stability experiment

All the above data suggests that based on strength reduction method, the mountain slope calculation model designed in this paper has an optimal stability analysis effect for the three kinds of slope types in mountains, and the weak interlining slopes in mountain have the best stability.

## 5. DISCUSSION

Through the research of this paper, the author thinks that it is necessary to further bring the strength reduction method into the actual use of reinforced concrete in the calculation of the stability safety index of mountain slopes, and maybe the seepage field can be simulated by the function of simulating the temperature field. Also, the author reckons that there are still several deficiencies in the case analysis of this paper. For instance, the influence of groundwater has not been considered and the

application of the various residual mountain slopes in the rock slopes is not studied, where only the shear damage of rock and soil structure is analyzed. In this regard, future research may create a subject aiming at the influence of groundwater on slope stability, and focus on the practical application of strength reduction calculation method in rock slopes on the basis of the tensile failure of rock and soil, the practical application of strength reduction calculation method in the safe and stable state analysis of foundations and underground caverns, and other practical applications from all walks of life. Moreover, how to use the strength reduction method to design the support structure in the foundation, cavern and slope is a also topic worthy of further study.

## 6. CONCLUSION

China is a mountainous country, where geological disasters such as landslides occur frequently every year, and losses caused thereupon are vitally massive. When carrying out landslide disaster management, it is the top priority of current mountain stability research to reasonably introduce relevant algorithms into the research on the stability of combined residual mountain slopes. Therefore, this paper proposes a strength reduction calculation model in the study of the stability of the residual mountains. And the following conclusions are drawn from the study:

1. The deformation and failure characteristics of the residual slope on the rear wall of a landslide in a certain area is analyzed. To be precise, from the distribution of three groups of fractures with different extension directions and scales formed on the surface of the residual mountain in a certain area, the vibration unloading effect is not only in the direction of the mouth of the river, but also in the direction of the big water ditch and the small water ditch. Collapse, sliding and cracking also occur, but the former has more advantages. Moreover, although the shallow surface layer of the residual mountain slope in a certain area is disturbed by the earthquake, the integrity of the underlying weakly weathered rock mass remains basically intact.
2. The stability of a multi-layer soil slope in a certain area in residual mountains via the method proposed in this paper, finite element limit equilibrium method, Bishop method and Janbu method is analyzed. It is found that the safety index obtained by the method proposed in this paper is 6.7%, 8.8%, and 10.5% higher than that calculated by other three methods in order.
3. The stability of a homogeneous slope in a certain area in residual mountains via the method proposed in this paper, finite element limit equilibrium method, Bishop method and Janbu method is analyzed. It is obvious that compared with other three methods, the safety index obtained by the method in this paper is increase by 4.8%, 4.3%, and 9.4% respectively. Similarly, in a weak interlining slope the safety index obtained by this method is 26.10%, 29.11%, and 26.46% higher than the other three methods successively, indicating that the stability of the landslide residual mountain calculated by the strength reduction method in this paper is the highest.

## 7. DATA AVAILABILITY STATEMENT

The original contributions presented in the study are included in the article/ supplementary material, further inquiries can be directed to the corresponding author.

## REFERENCES

- (1) Wei W B, Cheng Y M. (2019). **Stability analysis of slope with water flow by strength reduction method[J]**. *Soils & Foundations*, 50(1), 83-92.
- (2) Chen J F, Liu J X, Xue J F. (2017). **Stability analyses of a reinforced soil wall on soft soils using strength reduction method[J]**. *Engineering Geology*.
- (3) Wang L Y, Chen W Z, Tan X Y. (2019). **Evaluation of mountain slope stability considering the impact of geological interfaces using discrete fractures model[J]**. *Journal of Mountain Science*, 16(9), 2184-2202.
- (4) Wang Y, Jiang W, Li B. (2021). **Deformation Monitoring and Evaluation of Mountain Slope Stability Combined With Ground-based Radar and Spaceborne InSAR Methods**.
- (5) Xin Z, Han J, Zhuoyang L I. (2020). **Viability of high-density resistivity method for evaluating mountain slope stability in Erdaojiang District, Tonghua City, China[J]**. *World Geology: English Edition*.
- (6) Pingkang Wang, Youhai Zhu, Zhenquan Lu, Xia Huang, Shouji Pang and Shuai Zhang. (2017). **Gas hydrate stability zone migration occurred in the Qilian mountain permafrost, Qinghai, Northwest China: Evidences from pyrite morphology and pyrite sulfur isotope[J]**. *Cold Regions Science and Technology*.
- (7) Wang L Y, Chen W Z, Tan X Y. (2019). **Evaluation of mountain slope stability considering the impact of geological interfaces using discrete fractures model[J]**. *Journal of Mountain Science: English Edition*, 16(9), 19.
- (8) Xue F, Wang X. (2018). **Study on stability of the Santai Mountain landslide based on FLAC~(3D) numerical simulation[C]**. *2018 International Conference on Computational Science and Engineering*.
- (9) Liu W. (2018). **Study on foundation stability of a mountain project in Tianjin Binhai district[J]**. *IOP Conference Series Materials Science and Engineering*, 452(3), 032060.
- (10) Jian H, Zuo D, Xiao J. (2018). **Fast Evaluation and Application Study for Road Slope Stability in Mountain Area Based on Android Platform[J]**. *Safety and Environmental Engineering*.
- (11) Wang H. (2017). **Study on stability of high and steep slope in mountain reservoir[J]**. *Building Structure*.
- (12) Dong T W, Zheng Y R, Huang L Z. (2018). **Study of Ultimately Loading of Pile Foundation by Strength Reduction Method of No-Linear Limit Analysis of FEM[J]**. *Advanced Materials Research*, 168-170, 2537-2542.
- (13) Simatupang P T, Ohtsuka S. (2018). **Static and Seismic Slope Stability Analyses Based on Strength Reduction Method[J]**. *Doboku Gakkai Ronbunshuu A*, 3, 235-246.

- (14) Chen L, Jin X. (2019). **Study on the applicability of three criteria for slope instability using finite element strength reduction method[J]**. *China Civil Engineering Journal*, 45(9), 136-146.
- (15) Ying K, Chen P, Yu H. **Analysis of Rock High-Slope Stability Based on a Particle Flow Code Strength Reduction Method[J]**. *Electronic Journal of Geotechnical Engineering*, 20(28), 13421-13430.
- (16) Abbas F, Zhu Z, An S. (2021). **Evaluating aggregate stability of soils under different plant species in Ziwuling Mountain area using three renowned methods[J]**. *Catena*, 207(15), 105616.
- (17) Wang S, Li X C, Shi L. (2017). **Material point strength reduction method and its application to slope engineering[J]**. *Rock and Soil Mechanics*.
- (18) Chen G Q, Huang R Q, Zhou H. (2017). **Research on progressive failure for slope using dynamic strength reduction method[J]**. *Yantu Lixue/Rock and Soil Mechanics*.
- (19) Sheng-Dong X U, Zhang X, Zhang J. (2017). **Stability analysis of multi-step slope based on strength reduction method[j]**. *Journal of Geological Hazards and Environment Preservation*.
- (20) Schneider-Muntau, Barbara, Medicus. (2018). **Strength reduction method in Barodesy[J]**. *Computers & Geotechnics*.
- (21) Sun Y, Duan X R, Xu P H. (2021). **Reliability analysis of karst roof stability based on strength reduction method[J]**. *IOP Conference Series: Earth and Environmental Science*, 861(7), 072118(8).
- (22) Yunjin H U, Zhong Z, Gao H. (2021). **Three-parameter strength reduction method for slope stability evaluation.**
- (23) Zhang Zhewen, Gao Huaxi. (2019). **Effect of repressive layer on stability of seawall based on strength reduction method[J]**. *Water Transport Engineering*, 000(006), 180-185.
- (24) Shan, Shan, LU. (2018). **Dynamic Stability Analysis of Arch Dam Abutment Based on Strength Reduction Method[C]**.
- (25) Ying K, Chen P, Yu H. (2018). **Analysis of Rock High-Slope Stability Based on a Particle Flow Code Strength Reduction Method[J]**. *Electronic Journal of Geotechnical Engineering*, 20(28), 13421-13430.
- (26) Tulu I B, Esterhuizen G S, Klemetti T. (2016). **A case study of multi-seam coal mine entry stability analysis with strength reduction method[J]**. *International Journal of Mining Science and Technology*.
- (27) Bai B, Yuan W, Shi L. (2017). **Comparing a new double reduction method to classic strength reduction method for slope stability analysis[J]**. *Rock and Soil Mechanics*, 36(5), 1275-1281.
- (28) Y Zhou, T Chen, J Deng. (2019). **Three-dimensional stability analysis of slope regions based on strength reduction method.**
- (29) Yang Y, Wang Y, Wu Y. (2017). **The effect of variable modulus elastoplastic strength reduction method on slope stability[J]**. *Electronic Journal of Geotechnical Engineering*, 20(1), 1-10.
- (30) Tu Y, Liu X, Zhong Z (2018). **New criteria for defining slope failure using the strength reduction method[J]**. *Engineering Geology*, 212, 63-71.

- (31) Schneider-Muntau B, Medicus G, Fellin W. (2017). **Strength reduction method in Barodesy[J]**. *Computers and Geotechnics*, 95, 57-67.
- (32) Tulu I B, Esterhuizen G S, Klemetti T. (2018). **A case study of multi-seam coal mine entry stability analysis with strength reduction method[J]**. *International Journal of Mining Science and Technology*.
- (33) Nie Z B, Zheng H, Zhang T. (2017). **Determination of slope critical slip surfaces using strength reduction method and wavelet transform[J]**. *Rock and Soil Mechanics*.
- (34) Hou W, University L. (2018). **Stability Analysis of Inhomogeneous and Multi-step Slope Based on Strength Reduction Method[J]**. *Subgrade Engineering*.
- (35) Wei Y, Xiao-Tian H, Xiao-Chun L I. (2017). **A strength reduction method considering reduction of strength parameters coordinating with deformation parameters[J]**. *Rock and Soil Mechanics*.
- (36) Yan C, Liu S Y, Xiao-Lei J I. (2018). **Research on a secondary sliding surface analysis approach based on strength reduction method[J]**. *Rock and Soil Mechanics*.
- (37) Maqache, N., y Swart, A., J. (2021). **Remotely measuring and controlling specific parameters of a PV module via an RF link**. *3C Tecnología. Glosas de innovación aplicadas a la pyme*, 10(4), 103-129. <https://doi.org/10.17993/3ctecno/2021.v10n4e40.103-129>
- (38) Shen Siqu. (2021). **Multi-attribute decision-making methods based on normal random variables in supply chain risk management**. *Applied Mathematics and Nonlinear Sciences*, 7(1), 719-728. <https://doi.org/10.2478/AMNS.2021.2.00147>.

## CONFLICT OF INTEREST

The authors declare that the research was conducted in the absence of any commercial or financial relationships that could be construed as a potential conflict of interest.